

Short communication

A reliable technique to determine the local mechanical properties at the nanoscale for cementitious materials

Paramita Mondal^{a,*}, Surendra P. Shah^a, Laurence Marks^b

^a Center for ACBM, Department of Civil Engineering, Northwestern University, IL 60208, USA

^b Department of Materials Science and Engineering, Northwestern University, IL 60208, USA

Received 22 March 2006; accepted 4 July 2007

Abstract

A Hysitron Triboindenter has been used to determine the mechanical properties of hardened cement paste and cement paste at the early age. This technique provides an *in-situ* scanning probe microscopy (SPM) imaging facility that allows pre and post-test observation of the sample. The same probe is used to indent and image eliminating the complicated situation of locating the same area with different instruments or coupling two different instruments, such as a SEM and a nanoindenter to work together. This paper presents preliminary results of experiments performed on hardened cement paste and cement paste at the early age.

© 2007 Elsevier Ltd. All rights reserved.

Keywords: AFM; Cementitious materials; Nanostructure; Mechanical properties; Nanoindentation

1. Introduction

It is widely believed that the fundamental properties of concrete such as strength, ductility, early age rheology, creep and shrinkage, fracture behavior, durability, etc are affected by material properties at the nanoscale [1]. However, the nano- and the micro-scale structure of the most important hydration product in cement paste, calcium silicate hydrate (C–S–H), is not well established. In order to improve cement and concrete properties, it is necessary to understand the nanoscale structure and how this relates to the properties such as the local mechanical properties. So one needs to be able to both image the material, as well as determine for instance the Young's modulus of a given area or nanoscale feature in a fairly rapid fashion.

Many electron-beam imaging techniques exist and have been applied to cementitious materials, but by themselves they will not provide mechanical properties. In principle a local probe such as atomic force microscopy (AFM) [2] can, and it is just starting to be exploited to study the nanostructure of

cementitious materials [3–9]. As some examples, AFM has been used to study the surface changes of cement clinker immersed initially in saturated calcium hydroxide solution, followed by water, and sucrose solution [3]; the change in hydrated cement paste microstructure with the exposure to different humidity levels [4]; the carbonation process of calcium hydroxide present in the hydrated cement paste [5] and for imaging the denser microstructure of the cement paste with silica fume or fly ash [6]. One advantage of AFM is that it can be used with a special diamond indenter probe to extract nanoscale local mechanical properties along with high resolution imaging. This has been successfully implemented for different soft materials [10], but in general it only provides qualitative information and proportional values for the elastic modulus [11,12]. A different type of local probe, nanoindentation, has proved to be a reliable technique to quantitatively determine local mechanical properties [13–20]. The disadvantage

Table 1
Chemical compositions of Portland cement Type I — Lafarge

Chemical data	SiO ₂	CaO	Al ₂ O ₃	Fe ₂ O ₃	C ₃ S	C ₃ A
Percent	20.4	65.3	4.8	2.8	68	8

* Corresponding author. Tel.: +1 847 491 7161; fax: +1 847 467 1078.

E-mail address: paramita@northwestern.edu (P. Mondal).

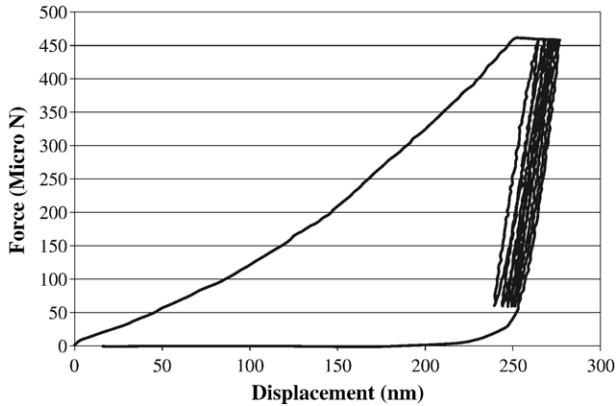


Fig. 1. Load displacement plot captured from nanoindentation on C–S–H in hardened cement paste sample.

of nanoindentation is the absence of any imaging ability which is an issue for heterogeneous materials such as cement paste. To overcome this problem, in some recent nanoindentation studies, a large number of indentations were performed on hydrated cement paste sample and the calculated modulus values were grouped statistically to get the modulus of different phases present [15,16]. In order to make the experiment more reliable, a cold field emission scanning electron microscope (CFE-SEM) has also been used to add an imaging capability in another study [18].

In this note we report results using a relatively new type of instrument which combines nanoindentation to determine the local mechanical properties at the nanoscale with high resolution *in-situ* scanning probe microscopy (SPM) imaging that allows pre and post-test observation of the sample; this instrument, the “Triboindenter”, has recently become commercially available. The ability to indent and image using the same probe in one instrument eliminates the complicated problem of locating the same area with different instruments or coupling two different instruments, such as a SEM and a nanoindenter to work together. This feature provides the capa-

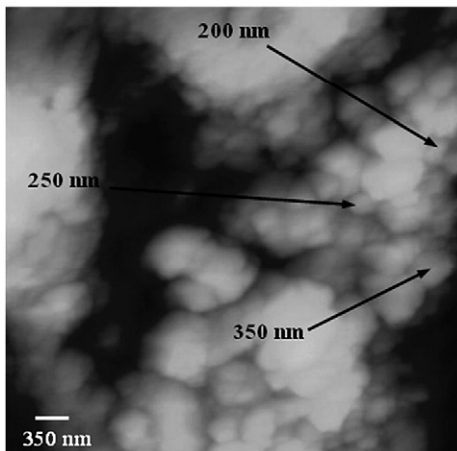


Fig. 2. 4.7 $\mu\text{m} \times 4.7 \mu\text{m}$ AFM image (topography) of C–S–H gel.

Table 2

Preliminary results of indentation where E is elastic modulus and H is hardness all in GPa

Unhydrated particle	High stiffness C–S–H		Medium stiffness C–S–H		Low stiffness C–S–H			
	E	H	E	H	E	H		
Mean	122.20	6.67	41.45	1.43	31.16	1.22	22.89	0.93
S.D.	7.85	1.23	1.75	0.29	2.51	0.07	0.76	0.11

bility to position the indenter probe within ten nanometers of the desired test location; a level of precision difficult to achieve with instruments that rely on stages to translate the sample from the optics or SPM to the probe position. Post-test imaging also provides the ability to verify that the test was performed in the anticipated location, which maximizes the reliability of the data. This paper presents preliminary results of experiments performed on hardened cement paste and cement paste at the early age.

2. Experimental details

For this preliminary study, we started our experiments with three years old cement paste sample that was readily available. These samples were prepared for a different project using ordinary Type I Portland cement provided by Lafarge. The chemical composition of the cement is listed in Table 1. The Blaine surface area was 365 m^2/kg . The specification of ASTM standard C305 was followed during the mixing of cement paste. Samples with water to cement ratio of 0.45 were prepared, and cured under water for a month at 25 °C temperature. After the curing period, samples were stored under general laboratory condition.

For microstructural characterization of the cement paste sample, specimens were cut and polished on silicon carbide papers down to 6.5 μm , then polished using diamond suspension down to 0.1 μm to obtain a very smooth surface. (Sample preparation is a very important step in this study since getting an extremely smooth surface is critical for the imaging and the reliable determination of local mechanical properties.)

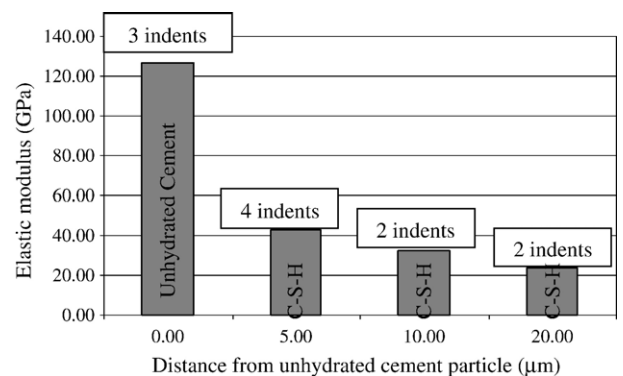


Fig. 3. Change in modulus of C–S–H with the distance from unhydrated particle.

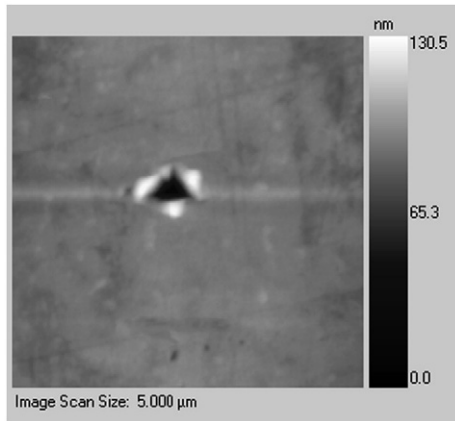


Fig. 4. Image of unhydrated cement particle recorded with cube corner tip in Triboindenter after indentation.

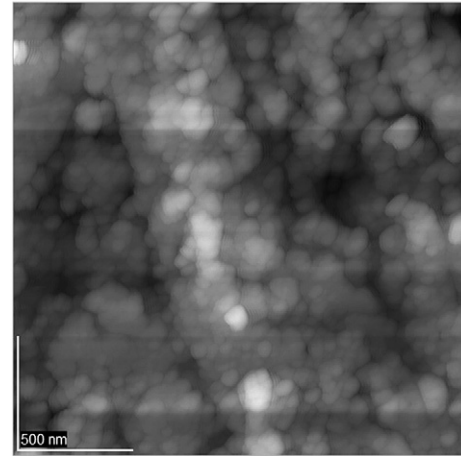


Fig. 6. 2 μm × 2 μm AFM image (topography) after 24 h of casting.

In between the polishing steps, an optical microscope was used to check the effectiveness of each step. At the end of polishing, a Quanta environmental scanning electron microscope was used at low vacuum mode to get an overall idea of the sample surface, examine the effectiveness of sample preparation and locate representative area on the sample surface. Two different Atomic Force Microscopes (AFM), a Digital Instrument (DI) Nanoscope MultiMode Scanning Probe Microscope and a JEOL JSPM-5200 were used in this study to provide structural and morphological information at the nanoscale. A Hysitron Triboindenter was used to determine the nanomechanical properties. Both a Berkovich tip with total included angle of 142.3° and a cube corner tip of total included angle of 90° were used for indentation in this study; the cube corner tip was found to be more effective in high resolution imaging because of the smaller included angle. The indenter tip itself can be used to capture AFM image of a sample. Since the tip radius of the two indenter tip mentioned above is in the range of 100–200 nm, image resolution is not as high as images from JEOL or DI AFM (tip radius typically in the range of 5–15 nm). Images of same area from SEM and JEOL or DI AFM were compared

with AFM images captured with the indenter tip to establish the protocol of identifying different phases of cement paste using the Triboindenter only. Once good correlation was established, the experimental steps mentioned below were followed using the Triboindenter:

1. Place cement paste sample and do initial setup of the instrument.
2. Identify desired test location with the high resolution optical microscope attached to the Triboindenter.
3. Image the desired test location (maximum area being $60\ \mu\text{m} \times 60\ \mu\text{m}$) in AFM mode using the indenter tip. This step involves, software controlled movement of the sample from the high resolution optical microscope to the Piezo with the transducer and indenter tip assembly.
4. Select test locations for nanoindentation on different phases captured in the image. This step involves just positioning the cursor on the image and software can save the x and y coordinates of the point with a mouse click. Since moving the tip to the indentation location is controlled by the Piezo, it is extremely precise.

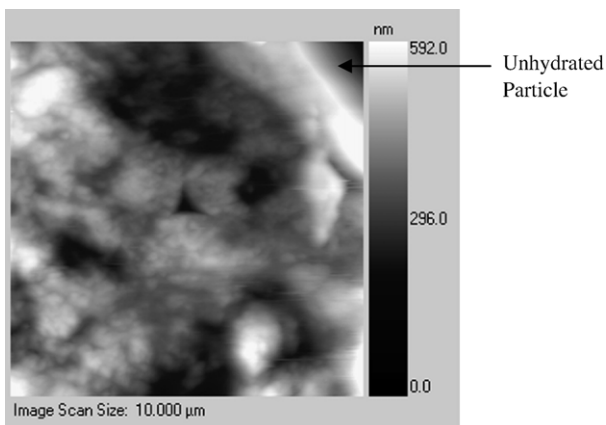


Fig. 5. 10 μm × 10 μm image of gel near unhydrated particle recorded with cube corner tip in Triboindenter after indentation.

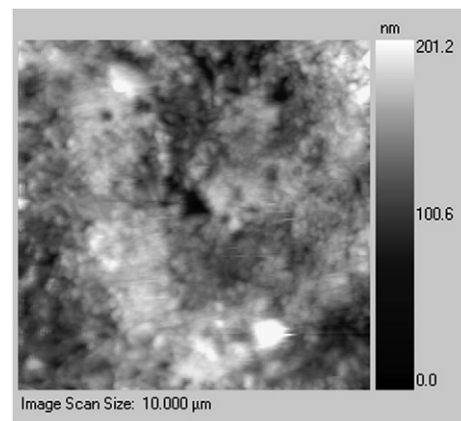


Fig. 7. 10 μm × 10 μm image recorded with cube corner tip in Triboindenter after indentation.

5. Make indent with specified maximum load and loading rate. Generally multiple cycles of partial loading and unloading was used to make every indent eliminating the creep effects and the size effects [20].

Fig. 1 shows a typical load displacement plot recorded from nanoindentation on C–S–H in hardened cement paste sample. In different tests, maximum load used for indentation on C–S–H was varied from 500 μN to 1500 μN at a loading rate of 100 $\mu\text{N/s}$ to 300 $\mu\text{N/s}$. Corresponding variation in depth of indentation was from 250 nm to 500 nm. Elastic properties were evaluated using the Oliver and Pharr method [13] from the final unloading region of the load vs. indentation curve.

Also the possibility of extending this technique to characterize the nanoscale properties of cement paste at the early age was checked. Since cement paste at the early age is too soft for a polishing approach, a different sample preparation method was used. Ordinary Type I Portland cement provided by Lafarge was used to make cement paste samples of water to cement ratio of 0.45. Samples were cast in small sample holders that fit both into the AFM and the Triboindenter and cured at 100% humidity and 25 °C for 24 h. A scanning electron microscope was used to locate well hydrated smooth areas on the surface that were later imaged with the AFM and mechanical properties were determined using the Triboindenter.

3. Results

Images of C–S–H in hardened cement paste show nearly spherical particles of different sizes in different areas. Typical sizes of these spherical particles range from 100 nm to 700 nm. Fig. 2 is a 4.7 $\mu\text{m} \times 4.7 \mu\text{m}$ AFM image of C–S–H gel with brighter regions being higher than darker ones. Maximum height difference between two different points in the image is 500 nm and image roughness is 56 nm. The image clearly shows particles of size 200 nm to 350 nm. To determine the local mechanical properties, several indentations were performed on different areas of C–S–H and on unhydrated cement particles. Table 2 shows the preliminary results of nanoindentation using a cube corner tip where elastic modulus values were determined with an assumed Poisson's ratio of 0.24 for all the phases. It was found that the elastic modulus can be divided in three different groups where values are decreasing with the distance from the unhydrated particle as shown in Fig. 3. Figs. 4 and 5 show the images of different areas recorded with the same cube corner tip after indentation. This illustrates the ability of this technique to identify different phases of the hydrated cement paste through imaging and determine the local mechanical properties of these phases.

Our initial results also demonstrated success in the study of cement paste at the early age. Fig. 6 shows one AFM image (topography) of C–S–H after 24 h of casting. The image shows nearly spherical particles of several tens of nanometers in size. Fig. 7 shows the image after indentation and the elastic modulus calculated after 24 h of hydration is 6 GPa. More experiments need to be performed at different ages to understand the changes in the nanostructure of cement paste during the hydration process.

4. Discussion

The technique described in this paper proved to be effective in determining the local mechanical properties at the nanoscale with concurrent imaging. The modulus and the hardness values calculated for unhydrated cement particles compare well with those of pure constituents of Portland cement clinker as reported by Velez et al. [17]. Results of indentation test on C–S–H are also within the range of the modulus and the hardness values reported in the literature [15,16, and 18]. Although the image resolution of a Triboindenter is not as high as a conventional AFM, it is possible to attribute the local mechanical properties to individual phases thereby eliminating the ambiguity that might exist in the nanoindentation data. Further research is underway to obtain precise characterization of cementitious materials at the nanoscale.

Acknowledgement

This research was performed as part of Federal Highway Administration Grant (Award No. DTFH61-05-C-0001).

References

- [1] D. Corr, S.P. Shah, Concrete materials science at the nanoscale, Applications of Nanotechnology in Concrete Design, Proceedings of the International Conference at the University of Dundee, Scotland UK, Thomas Telford, July 2005, pp. 1–12.
- [2] G. Binnig, C.F. Quate, C. Gerber, Atomic force microscope, Physical Review Letters 56 (9) (1986).
- [3] L.D. Mitchell, M. Prica, J.D. Birchall, Aspects of Portland cement hydration studied using atomic force microscopy, Journal of Materials Science 31 (1996) 4207–4212.
- [4] T. Yang, B. Keller, E. Magyari, AFM investigation of cement paste in humid air at different relative humidities, Journal of Physics D, Applied Physics 35 (2002) L25–L28.
- [5] T. Yang, B. Keller, E. Magyari, K. Hametner, D. Günther, Direct observation of the carbonation process on the surface of calcium hydroxide crystal in hardened cement paste using Atomic Force Microscope, Journal of Materials Science 38 (2003) 1909–1916.
- [6] V.G. Papadakis, E.J. Pedersen, H. Lindgreen, An AFM-SEM investigation of the effect of silica fume and fly ash on cement paste microstructure, Journal of Materials Science 34 (1999) 683–690.
- [7] A. Kauppi, K.M. Andersson, L. Bergström, Probing the effect of superplasticizer adsorption on the surface forces using the colloidal probe AFM technique, Cement and Concrete Research 35 (2005) 133–140.
- [8] A. Nonat, The structure and stoichiometry of C–S–H, Cement and Concrete Research 34 (2004) 1521–1528.
- [9] C. Plassard, E. Lesniewska, I. Pochard, A. Nonat, Investigation of the surface structure and elastic properties of calcium silicate hydrates at the nanoscale, Ultramicroscopy 100 (3–4) (2004) 331–338.
- [10] C. Reynaud, F. Sommer, C. Quet, C. El Bounia, T.M. Duc, Quantitative determination of Young's modulus on a biphasic polymer system using atomic force microscopy, Surface and Interface Analysis 30 (2000) 185–189.
- [11] M.S. Bishel, M.R. Vanlandingham, R.F. Eduljee Jr., J.W. Gillespie, J.M. Schultz, On the use of nanoscale indentation with the AFM in the identification of phases in blends of linear low density polyethylene and high density polyethylene, Journal of Materials Science 35 (1) (2000) 221–228.
- [12] M.R. Vanlandingham, S.H. McKnight, G.R. Palmese, R.F. Eduljee Jr., J.W. Gillespie, R.L. McCulough, Relating elastic modulus to indentation response using atomic force microscopy, Journal of Materials Science Letters 16 (2) (1997) 117–119.

- [13] W.C. Oliver, G.M. Pharr, An improved technique for determining hardness and elastic modulus using load and displacement sensing indentation experiments, *Journal of Material Research* 7 (1992) 1564–1583.
- [14] Fischer-Cripps, C. Anthony, *Nanoindentation*, Secaucus, NJ USA, Springer-Verlag, New York.
- [15] G. Constantinides, F.J. Ulm, The effect of two types of C–S–H on the elasticity of cement-based materials: Results from nanoindentation and micromechanical modeling, *Cement and Concrete Research* 34 (2004) 67–80.
- [16] G. Constantinides, F.J. Ulm, K. Van Vliet, On the use of nanoindentation for cementitious materials, *Materials and Structures/Materiaux et Constructions* 36 (257) (2003) 191–196.
- [17] K. Velez, S. Maximilien, D. Damidot, G. Fantozzi, F. Sorrentino, Determination by nanoindentation of elastic modulus and hardness of pure constituents of Portland cement clinker, *Cement and Concrete Research* 31 (2001) 555–561.
- [18] J.J. Hughes, P. Trtik, Micro-mechanical properties of cement paste measured by depth-sensing nanoindentation: a preliminary correlation of physical properties with phase type, *Materials Characterization* 53 (2–4) (2004) 223–231.
- [19] W. Zhu, M. Sonebi, P.J.M. Bartos, Bond and interfacial properties of reinforcement in self-compacting concrete, *Materials and Structures/Materiaux et Constructions* 37 (2004) 442–448.
- [20] J. Nemecek, L. Kopecky, Z. Bittnar, Size effect in nanoindentation of cement paste, applications of nanotechnology in concrete design, *Proceedings of the International Conference at the University of Dundee, Scotland UK, Thomas Telford, July 2005*, pp. 47–53.